Available online at www.sciencedirect.com
SCIENCE DIRECT®
Chemical Physics 285 (2002) 39–45
Chemical Physics
www.elsevier.com/locate/chemphys

Observation of photoinduced electron transfer in dye/semiconductor colloidal systems with different coupling strengths

Robert Huber[a], Jacques E. Moser[b], Michael Grätzel[b], Josef Wachtveitl[a,*]

[a] *Lehrstuhl für BioMolekulare Optik, Oettingenstr. 67, Ludwig-Maximilians-Universität München, 80538 München, Germany*
[b] *Laboratory for Photonics and Interfaces, Department of Chemistry, Ecole Polytechnique Fédérale de Lausanne, CH-1015 Lausanne, Switzerland*

Received 12 December 2001

Abstract

Investigations on the ultrafast electron injection and recombination mechanism from the dyes alizarin and coumarin 343 to wide band gap semiconductor colloids in solution are presented, combined with detailed studies on population, depopulation and relaxation phenomena. We discuss transient absorption measurements on time scales from 100 fs to >1 ns throughout the visible spectral range (350–650 nm), allowing the simultaneous time resolved observation of signals assigned to ground state, cation and injected electron in the conduction band of the semiconductor. Analysis of transient absorption changes in the near UV region, where cation absorption is dominant, allows unambiguous assignment of the various kinetic components. This facilitates the distinction between the different contributions of the various absorbing species also in the congested visible spectral range. Comparison between the two dyes with respect to their different electron transfer parameters provides a direct way to analyze the influence of the electronic coupling element V on the injection and recombination process. Detailed inspection of the decay related spectra for both samples yields information on the environmental response succeeding the cation formation.

1. Introduction

Sensitization of wide band gap semiconductors by organic dye molecules is a well established technique with widespread applications like the photographic process, detoxification and purification of water [1], and solar energy to electricity conversion [2–9]. Considerable physical interest in these dye/semiconductor systems surely arises from the special energetic situation, allowing ultrafast electron transfer from a system with discrete energy levels on the donor side, into a continuum of energy levels on the acceptor side (see Scheme in Fig. 5). In our case the elementary reaction can be written as

* Corresponding author. Present address: Institut für Physikalische und Theoretische Chemie, Marie-Curie-Str. 11, Goethe-Universität Frankfurt, 60439 Frankfurt am Main, Germany. Fax: +49-69-798-29709.
E-mail addresses: JE.Moser@epfl.ch (J.E. Moser), wveitl@theochem.uni-frankfurt.de (J. Wachtveitl).

0301-0104/02/$ - see front matter
PII: S0301-0104(02)00687-0

$$S + h\nu \rightarrow S^* \rightarrow S^+ + e^-_{surf}(TiO_2)$$
$$\rightarrow S^+ + e^-_{CB}(TiO_2)$$

where the dye, attached to the colloidal surface is excited from the ground state S to the excited state S*, energetically situated above the conduction band edge of the semiconductor [10], the excited state S* acts as electron donor and electron transfer to surface states of the semiconductor and subsequently to the conduction (e_{cb}) band occurs [10–28]. The dye molecule remains as cation S^+. The back reaction and charge recombination to the ground state of the dye depends on the solvent, the presence/absence of electrolytes, the morphology of the TiO_2 and also on the amount of adsorbed cations on the semiconductor surface [29]. The time scales for the back reaction vary from sub-ps up to milliseconds [7,8,10,23,30–33]. The various reaction steps and the energetic situation are summarized in Fig. 5. A detailed theoretical treatment of interfacial electron transfer is complicated, since reliable molecular models for the interface are needed and the presence of surface states or structural inhomogeneities have to be considered. Whereas for weakly coupled systems injection times of 100 fs–10 ps were found, for systems with moderate to high electronic coupling strengths, the electron injection is reported to take place on a sub-100 fs time scale [10,22,23,27,33–37]. As reported in [10], trap states on the surface of the semiconductor play a crucial role for the injection process. The interaction between these states and the adsorbed dye molecule can be analyzed by variation of the dye molecule, changing the relevant electron transfer parameters of the system, e.g., the electronic coupling matrix element V.

2. Experimental section

Measurements were performed on samples containing alizarin and coumarin 343 coupled onto TiO_2 colloids in solution. The systems were diluted in methanol to final concentrations of 0.5 mM alizarin and 0.1 mM coumarin on 10 g/l TiO_2 colloids. The colloidal nanoparticles of TiO_2 were prepared as previously described [10]. For the transient absorption measurements we used a classical pump/probe setup. The pump pulses (attenuated to 0.5 μJ at 495 nm for the alizarin system and 0.1 μJ at 495 nm for the coumarin system) were provided by a non-collinear optical parametric amplifier (NOPA), pumped with 50 μJ pulses at 400 nm of the second harmonic of a home-built regenerative amplifier system (1 kHz, 1 mJ, 800 nm). The NOPA was seeded with a white light super continuum, generated in a calcium fluoride plate [38]. The resulting pulse to pulse energy fluctuations of the NOPA were less than 1% rms (at pulse to pulse energy fluctuations of the regenerative amplifier system at 800 nm of $<0.5\%$). The pulse duration of the NOPA output after compression was measured by a home-built intensity autocorrelator (second harmonic generation in a 25 μm thick BBO). The pulse compression of the NOPA pulses was performed by a standard prism compressor (SiO_2, 60°). The pulse duration of the compressed NOPA output was measured to be about 19 fs at a wavelength of 495 nm at the location of the sample. The diameter of the excitation spot inside the cuvette was 80 μm, the optical pathlength through the sample was 50 μm.

The probe pulses were provided by super continuum (SC) generation with about 3 μJ of the 800 nm fundamental of the regenerative amplifier in a CaF_2 plate. The generated single filament SC covers a spectral range from about 320 to >1000 nm with significant intensity of >80 nJ. The SC is imaged via all reflective optics into the sample with a focal diameter of 40–50 μm, depending on the wavelength. The cross correlation functions, determined by fitting the coherent signals at the delay time zeros [39], were found to be <35 fs for probing wavelengths between 374 and 630 nm and <50 fs for the rest of the investigated spectrum.

The analysis of the temporal evolution of the transient absorption spectra, especially the spectral assignment of the occurring transient species, was performed by a home-written software, supplying a fast Marquardt downhill algorithm for a global fit of the recorded data, optimizing simultaneously n global decay times for all transients.

3. Results

3.1. cw-Absorption/emission

Fig. 1 shows cw absorption and fluorescence data of the samples alizarin in solution, alizarin coupled on TiO_2, coumarin in solution and coumarin coupled onto TiO_2. The absorption band of alizarin shows a strong spectral shift of about 60 nm whereas for coumarin the shift in absorption is only about 20 nm. The plotted fluorescence spectra in Fig. 1 (bottom) are for free coumarin (squares) as well as for the coupled system (up triangles). The spectra are normalized, since the absolute quantum efficiency is quenched by a factor of 40 upon the coupling process for coumarin and a factor of >500 for the alizarin system. So we were not able to obtain a fluorescence spectrum of coupled alizarin, because residual fluorescence could not be clearly distinguished from residual fluorescence of remaining free alizarin in solution. For the coumarin system, the fluorescence peak is shifted about 50 nm upon the adsorption and the spectral shape of the emission band is about a factor 2 broader (80 nm compared to 40 nm). The slightly structured shape of the emission band is due to noise in the fluorescence measurement because of its low intensity. The absorption and the emission band of free coumarin in solution lie almost perfectly symmetric to each other whereas for the coupled coumarin system the fluorescence band is not only broader but also different in its spectral shape.

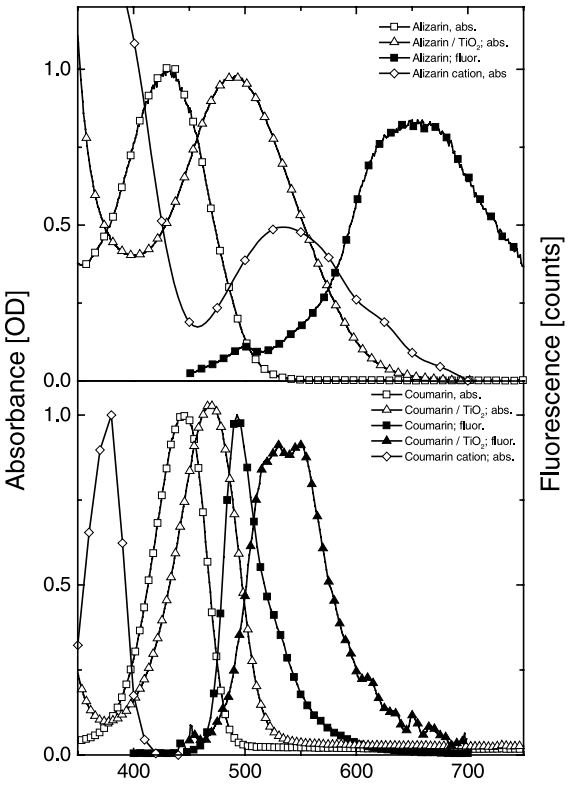

Fig. 1. (top) cw-Absorption spectra for free alizarin in solution (open squares), alizarin coupled onto TiO_2 (open up triangles), and the cation spectrum for the coupled alizarin (diamonds, calculated as described above); fluorescence spectrum of free alizarin (solid squares). (bottom) cw-Absorption spectra for free coumarin in solution (open squares), coumarin coupled onto TiO_2 (open up triangles), and the cation spectrum for the coupled coumarin (diamonds), calculated by spectral subtraction from ns transient absorption measurements; fluorescence of free coumarin (solid squares) and coupled coumarin (solid up triangles).

The spectrum of the coumarin-343 cation adsorbed on colloidal TiO_2 in water/ethanol (50:50 v/v) solvent mixture was calculated by spectral subtraction of the transient absorption spectrum recorded 100 ns after laser pulsed excitation of the adsorbed dye (5 ns pulse duration, $\lambda_{exc.} = 480$ nm) and the absorption spectrum of the dye ground state. Assuming the dye cation (S^+) has no absorption at wavelengths above 450 nm, the spectrum of this transient species $A(S^+)$ is obtained by subtracting the dye ground state bleaching signal from the original transient spectrum.

The spectrum of the alizarin cation (adsorbed on TiO_2) was also obtained by transient nanosecond spectroscopy. Spectral subtraction of the ground state absorption from the transient absorbance change at 1 μs, when the electron in the conduction band and the alizarin cation are supposed to be the only absorbing species, results in the cation spectrum (assuming that for wavelengths >700 nm only the electron in the conduction band contributes to the total absorption).

3.2. Transient absorption measurements

Fig. 2 shows transient absorption data of both investigated systems – alizarin on TiO_2 (left) and coumarin 343 on TiO_2 (right). For the alizarin

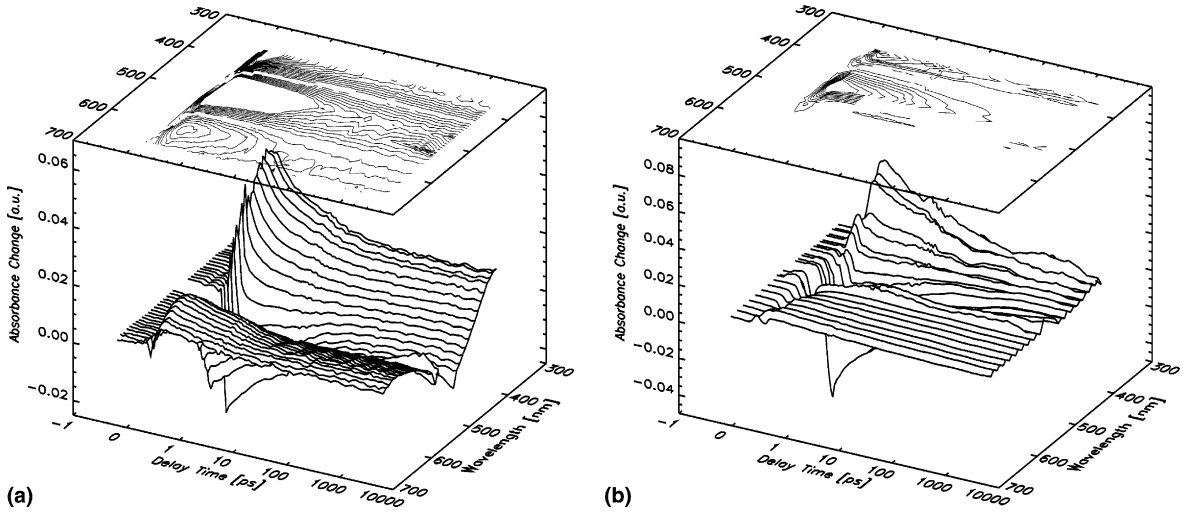

Fig. 2. Transient absorbance change after photoexcitation for alizarin on TiO_2 (left) and coumarin on TiO_2 (right).

system three dominant contributions can be distinguished as follows: for wavelengths <420 nm the transients show a positive difference absorption with increasing amplitude for shorter wavelengths. In the spectral region between 420 and 560 nm, transients with negative absorption are found and the long wavelength side of the presented data is again dominated by unstructured, positive transient absorbance changes. The observed dynamics is obviously spread over a temporal range from <1 ps to >1 ns.

Over the complete spectral range the maximum transient absorbance changes were observed instantaneously, i.e., within the temporal resolution of the presented measurements. Thus an upper limit of 100 fs for the formation of the difference spectrum can be given.

Analysis of the decay related spectra of the global fitting procedure reveals a synchronous monotonous decay of the initial difference spectrum in a multi-exponential way (Fig. 3). The spectral signature of the 4 decay related spectra resemble each other apart from a scaling factor. The remaining transient difference spectrum at delay times >3 ns is expressed by a fixed decay time with infinite value.

For the system coumarin 343 on TiO_2 the formation of the transient difference absorption occurs again instantaneously within the temporal resolution of the measurements as for the alizarin system (upper limit: 100 fs). Positive transient absorption can be found for wavelengths <400 nm,

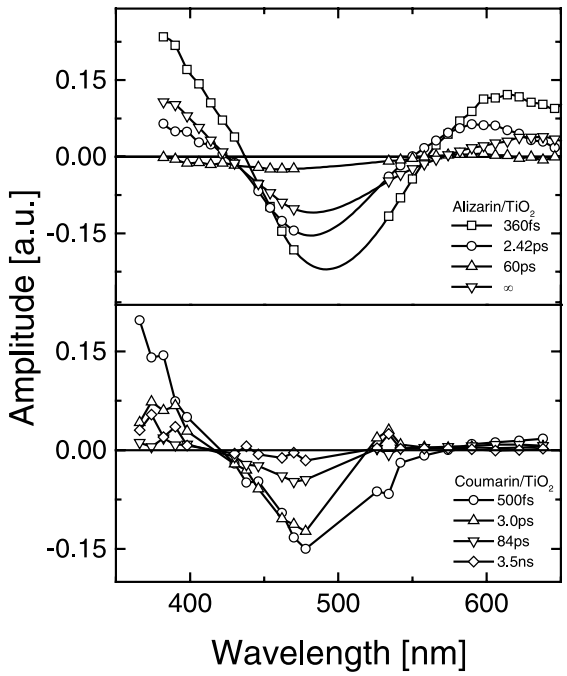

Fig. 3. Linear fitting amplitudes of the global fitting procedure as decay related spectra, for alizarin on TiO_2 (top) and coumarin on TiO_2 (bottom), connected by a spline curve.

monotonously decreasing with a kinetic components from <1 ps to 3 ns. In the region between 400 and 530 nm negative transient absorption with a temporal evolution from <1 ps to >3 ns can be observed. For the transients at wavelengths >600 nm a small unstructured positive absorption can be found (see figure, components 500 fs and 84 ps).

A comparison between the optimized time constants reveals a slight increase for the first three constants. The best fit constants for the alizarin systems are 120 fs, 360 fs, 60 ps, 2.4 ps and an infinite component, whereas for the coumarin system values of 500 fs, 3 ps, 84 ps and 3 ns were found. The amplitudes of the coumarin kinetics are significantly smaller for wavelengths >550 nm than for the alizarin system for all decay times.

4. Discussion

4.1. cw-Absorption/emission

The cw-spectra in Fig. 1 give a first indication for the electronic situation within the two investigated systems. The larger shift of the absorption band upon adsorption for the alizarin system reflects the higher electronic coupling, as discussed in [31].

The broader band shape of the emission spectrum for coumarin could be explained by heterogeneity of the environment around the docking site for different coumarin molecules as well as by an altered emitting energy level in the coupled systems. The fluorescence quenching by a factor of 40 for the coumarin system indicates the effective depopulation of the excited state. A quantitative analysis comparing this quenching factor to the transient absorption experiments, will be discussed below.

4.2. Transient absorption measurements for the strong coupling case: alizarin

Comparison between the cw-spectra (Fig. 1) and the transient data (Fig. 2) allows the spectral assignment of the recorded transient absorbance changes to the different species. For the alizarin system the mentioned three different spectral ranges in the transient absorption measurements can be assigned to: (a) cation absorption for wavelengths <420 nm, (b) ground state bleaching from 420 to 560 nm, overcompensating the minor contributions of cation absorption in this spectral range and (c) cation absorption combined with absorption of the injected electron for wavelength 560 nm and longer. At first glance, the shape of the decay related spectra reflects the dominance of ground state recombination over the whole investigated spectral range [10]. The requirement of several time constants for a satisfactory global fit expresses a highly non-exponential recombination reaction. For all time constants, the decay related spectra show almost the same signature, except the one for the 2.4 ps component at wavelengths >600 nm. Whereas all other spectra show a flat and unstructured shape, the 2.4 ps decay spectrum has a maximum at 600 nm and decreases towards longer wavelengths. Fig. 4 shows a plot of the decay related spectra, rescaled for wavelengths <420 nm. The good agreement of the 360 fs component and the long time offset (∞-component) underlines the multiphasic ground state recombination from hundreds of femtoseconds to >1 ns. The 2.4 ps component shows a significant deviation from this spectral shape. For a detailed analysis of this spectral feature and to discriminate between the involved reactions, the spectrum of the residual component (∞-component), assumed to be caused only by the bleached ground state, the

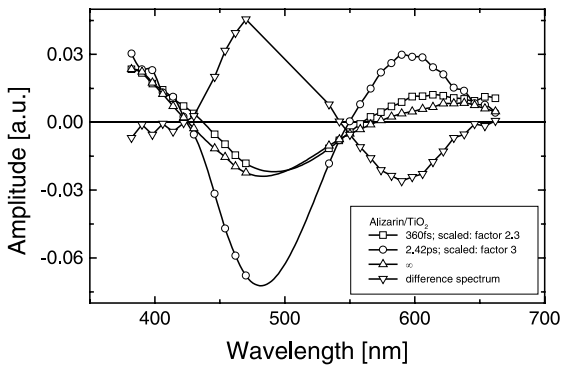

Fig. 4. Rescaled decay related spectra for the 360 fs (squares), 2.4 ps (circles) and the infinite time constant (up triangles), <420 nm. Difference spectrum between 2.4 ps component and infinite component (down triangles).

alizarin cation and the electron in the conduction band (Fig. 4, down triangles), was subtracted from the 2.4 ps decay spectrum. Fig. 4 (down triangles) shows the resulting difference spectrum. A possible reason for such a difference spectrum with a totally antisymmetric shape could be a dynamic shift of an absorption band. If a Gaussian shaped band structure is shifted in time, multi-exponential global fitting processes show such an antisymmetric signature (e.g. dynamic Stokes shift). The largest amplitudes are placed around the wings of the band, the zero crossing around its maximum. Comparison with the cw-absorption spectrum of the alizarin cation implies a dynamic shift of the cation absorption band towards the signature measured in the cw-experiment (ns-experiment). Remembering the upper limit for the electron injection of 100 fs, the 2.4 ps kinetic component could reflect solvent reorganization or relaxation processes within the semiconductor lattice succeeding the cation formation.

4.3. Transient absorption measurements for the moderate coupling case: coumarin

For a closer characterization of the decay related spectra in the coumarin system, the extinction coefficient ε for coumarin compared to alizarin must be taken into account. Therefore, transient absorption of the electron in the conduction band is much smaller in amplitude than the effect of the ground state bleaching and cation absorption. This is the reason that no signal can be observed for wavelengths >550 nm (Fig. 2, bottom).

Analogous to the spectral assignment of the alizarin system, the instantaneous rise of transient difference absorption at wavelengths <410 nm and >575 nm can be assigned to cation absorption and absorption of the electron in the conduction band, also implying an injection process faster than 100 fs. The slightly higher time constants observed in the coumarin system should be assigned to the same reaction steps. The remarkably good agreement of the 500 fs (300 fs) component and the 3 ps (2.4 ps) component indicate processes apart from the dye molecule and support the model of environmental relaxation or reorganization on a 3 ps time scale succeeding the cation formation as discussed above. An analogue analysis as for alizarin, and a discussion of a possible shift of the coumarin cation absorption band, is hindered by the small amplitudes at long wavelengths. The recombination ratio, taken from the transients at 374 nm (ratio between initial amplitude and long time offset; time constants: 3 ns for coumarin, ∞ for alizarin) with dominant absorption of the coumarin cation, was about 70% after 1 ns for coumarin. This is no significant deviation from values of 63–70% found for alizarin (at <400 nm and >600 nm), implying the electronic coupling plays a minor role for the back reaction in reactive dye/TiO_2 systems at least for dyes with moderate to strong electronic coupling matrix elements (see Fig. 5).

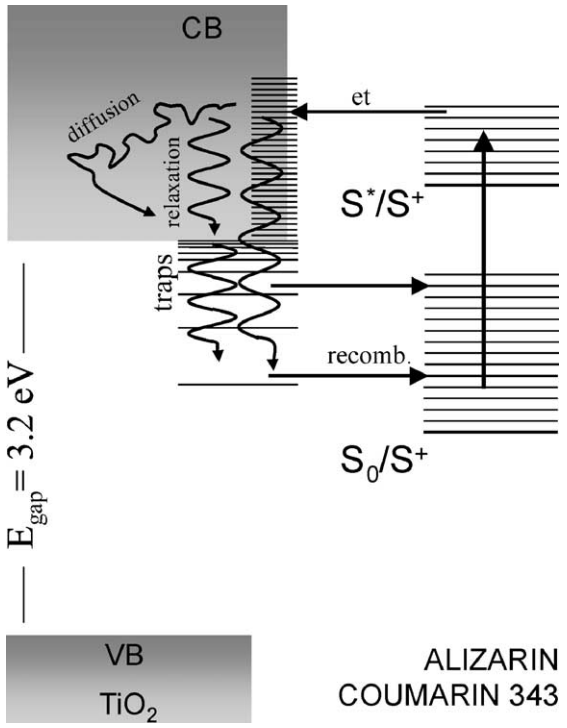

Fig. 5. Energetic situation for dye (alizarin, coumarin) adsorbed onto a TiO_2 colloid after photoexcitation.

5. Conclusions

The presented NOPA pump/SC probe setup, using a SC generated in CaF_2, allows the simultaneous observation of the characteristic spectral

features of the neutral and the positively charged dye as well as the electron in the conduction band for both investigated systems. The analysis of the presented transient absorption measurements on the coumarin/TiO_2 and the alizarin/TiO_2 system reveals a kinetic component additional to the ground state recombination, which can be explained by a spectral shift of the cation absorption, caused by the response of the solvent or the semiconductor. Analysis of the temporal evolution of both investigated systems resulted in a qualitative agreement of the observed time constants, suggesting a minor role of the electronic coupling for the back reaction.

Acknowledgements

The authors would like to thank W. Zinth for helpful discussions. This work is supported by the Deutsche Forschungsgemeinschaft (SFB 377/TP B10). JEM and MG are grateful to the Swiss National Science Foundation (FNRS) for financial support.

References

[1] T. Wu, G. Liu, J. Zhao, J. Phys. Chem. 103 (1999) 4862.
[2] A. Hagfeldt, U. Björksten, M. Grätzel, J. Phys. Chem. 100 (1996) 8045.
[3] B. O'Regan, D.T. Schwartz, J. Appl. Phys. 80 (1996) 4749.
[4] U. Bach, D. Lupo, P. Comte, J.E. Moser, F. Weissörtel, J. Salbeck, H. Spreitzer, M. Grätzel, Nature 395 (1998) 583.
[5] O. Enea, J. Moser, M. Grätzel, J. Electroanal. Chem. 259 (1989) 59.
[6] M.K. Nazeeruddin, A. Kay, I. Rodicio, R. Humphry-Baker, E. Müller, P. Liska, N. Vlachopoulos, M. Grätzel, J. Am. Chem. Soc. 115 (1993) 6382.
[7] M. Nazeeruddin, P. Liska, J. Moser, N. Vlachopoulos, M. Grätzel, Helv. Chim. Acta 73 (1990).
[8] B. O'Regan, J. Moser, M. Anderson, M. Grätzel, J. Phys. Chem. 94 (1990) 8720.
[9] B. O'Regan, M. Grätzel, Nature 353 (1991) 737.
[10] R. Huber, S. Sebastian, J.E. Moser, M. Grätzel, J. Wachtveitl, J. Phys. Chem. 104 (2000) 8995.
[11] J. Moser, M. Grätzel, D.K. Sharma, N. Serpone, Helv. Chim. Acta 24 (1985) 1686.
[12] J. Moser, M. Grätzel, J. Am Chem. Soc. 106 (1984) 6557.
[13] M. Hilgendorff, V. Sundstrom, Chem. Phys. Lett. 287 (1998) 5.
[14] M. Hilgendorff, V. Sundström, J. Phys. Chem. B 102 (1998) 10505.
[15] T.A. Heimer, E.J. Heilweil, J. Phys. Chem. 101 (1997) 10990.
[16] H.N. Ghosh, J.B. Asbury, T. Lian, J. Phys. Chem. 102 (1998) 6482.
[17] H.N. Ghosh, J.B. Asbury, Y. Weng, T. Lian, J. Phys. Chem. 102 (1998) 10208.
[18] Y. Tachibana, J.E. Moser, M. Grätzel, D.R. Klug, J.R. Durrant, J. Phys. Chem. 100 (1996) 20056.
[19] R.J. Ellingson, J.B. Asbury, S. Ferrere, H.N. Ghosh, J.R. Sprague, T. Lian, A.J. Nozik, J. Phys. Chem. 102 (1998) 6455.
[20] T. Hannappel, B. Burfeindt, W. Storck, J. Phys. Chem. 101 (1997) 6799.
[21] T. Hannappel, C. Zimmermann, B. Meissner, B. Burfeindt, W. Storck, F. Willig, J. Phys. Chem. 102 (1998) 3651.
[22] B. Burfeindt, T. Hannappel, W. Storck, F. Willig, J. Phys. Chem. 100 (1996) 16463.
[23] J. Wachtveitl, R. Huber, S. Spörlein, J.E. Moser, M. Grätzel, J. Photoenerg. 1 (1999) 153.
[24] P.V. Kamat, Prog. Reaction Kinetics 19 (1994) 277.
[25] R. Argazzi, C.A. Bignozzi, T.A. Heimer, F.N. Castellano, G.J. Meyer, J. Phys. Chem. 101 (1997) 2591.
[26] I. Martini, G.V. Hartland, J. Phys. Chem. 100 (1996) 19764.
[27] I. Martini, J. Hodak, G.V. Hartland, J. Chem. Phys. 107 (1997) 8064.
[28] I. Martini, J.H. Hodak, G.V. Hartland, J. Phys. Chem. 102 (1998) 607.
[29] S. Pelet, J.E. Moser, M. Grätzel, J. Phys. Chem. B 104 (2000) 1791.
[30] J.E. Moser, Solar Energy Materials Solar Cells 38 (1995) 1.
[31] J.E. Moser, M. Grätzel, Chem. Phys . 176 (1993) 493.
[32] S.A. Haque, Y. Tachibana, D.R. Klug, J.R. Durrant, J. Phys. Chem. 102 (1998) 1754.
[33] R. Huber, S. Spörlein, J.E. Moser, M. Grätzel, J. Wachtveitl, in: T. Elsaesser, S. Mukamel, M.M. Murnane, N.F. Scherer (Eds.), Ultrafast Phenomena XII, Springer, Berlin, 2000, pp. 456–458.
[34] J.B. Asbury, E. Hao, Y. Wang, H.N. Ghosh, T. Lian, J. Phys. Chem. B 105 (2001) 4545.
[35] J.M. Rehm, G.L. McLendon, Y. Nagasawa, K. Yoshihara, J. Moser, M. Gratzel, J. Phys. Chem. 100 (1996) 9577.
[36] J. Kallioinen, V. Lehtovuori, P. Myllyperkio, K. Korppi-Tommola, Chem. Phys. Lett. 340 (2001) 217.
[37] B. Burfeindt, C. Zimmermann, S. Ramakrishna, T. Hannappel, B. Meissner, W. Storck, F. Willig, Z. Phys. Chem. 212 (1999) 67.
[38] R. Huber, H. Satzger, W. Zinth, J. Wachtveitl, Opt. Commun. 194 (2001) 443.
[39] S.A. Kovalenko, A.L. Dobryakov, J. Ruthmann, N.P. Ernsting, Phys. Rev. A 59 (1999) 2369.